Title
Infrared nanospectroscopy characterization of metal oxide photoresists

Journal
Journal of Micro/Nanopatterning Materials and Metrology, 21(4)

ISSN
1932-5150

Authors
Zhao, Xiao
Wu, Cheng Hao
Bechtel, Hans A
et al.

Publication Date
2022-10-01

DOI
10.1117/1.jmm.21.4.041408

Infrared nanospectroscopy characterization of metal oxide photoresists

Xiao Zhao[a,b] **Cheng Hao (Will) Wu**[c,*] **Hans A. Bechtel**[d] **Timothy Weidman**[c] **and Miquel B. Salmeron**[a,b,*]

[a]University of California, Berkeley, Department of Materials Science and Engineering, Berkeley, California, United States

[b]Lawrence Berkeley National Laboratory, Material Science Division, Berkeley, California, United States

[c]Lam Research Corporation, Fremont, California, United States

[d]Lawrence Berkeley National Laboratory, Advanced Light Source, Berkeley, California, United States

Abstract. Implementation of extreme ultraviolet (EUV) lithography in high-volume semiconductor manufacturing requires a reliable and scalable EUV resist platform. A mechanistic understanding of the pros and cons of different EUV resist materials is critically important. However, most material characterization methods with nanometer resolution use an x-ray photon or electron beam as the probe, which often cause damage to the photoresist film during measurement. Here, we illustrated the use of non-destructive infrared nanospectroscopy [or nano-Fourier-transform infrared spectroscopy (nano-FTIR)] to obtain spatially resolved composition information in patterned photoresist films. Clear evidence of exposure-induced chemical modification was observed at a spatial resolution down to 40 nm, well below the diffraction limit of infrared light. With improvements, such a nano-FTIR technique with nanoscale spatial resolution, chemical sensitivity, and minimal radiation damage can be a promising candidate for the fundamental study of material properties relevant to EUV lithography.

Keywords: extreme ultraviolet photoresist; metal cluster photoresist; nano-Fourier-transform infrared spectroscopy; spectromicroscopy.

1 Introduction

Extreme ultraviolet (EUV) lithography is now established as the leading-edge technology for next-generation lithography, but widespread introduction and implementation of EUV lithography has been delayed partly by the lack of reliable and scalable photoresist platforms. Factors such as strong ionizing interaction between EUV light and all elements, EUV photon stochastics, and etch resistance necessary for robust pattern transfer all impose stringent requirements on the EUV photoresist.[1] Understanding the physical and chemical properties of EUV photoresists and their interactions with EUV photons as well as secondary electrons is critically important for photoresist design and optimization, particularly at the length scale relevant to the feature size in next-generation devices, typically a few nanometers.

Material characterization techniques able to reach nanometer resolution, including spectroscopy and microscopy techniques, typically use highly energetic probes such as x-ray photon and electron beams. The most widely used metrology techniques in the semiconductor industry include various electron microscopies such as scanning electron microscope (SEM) and transmission electron microscope (TEM)/scanning transmission electron microscope (STEM), along with spectroscopies that are part of the instrument such as energy-dispersive x-ray spectroscopy (EDS) and electron energy loss spectroscopy (EELS). Resist materials are designed to be highly

*Address all correspondence to Cheng Hao (Will) Wu, will.wu@lamresearch.com; Miquel B. Salmeron, mbsalmeron@lbl.gov

sensitive to high energy excitations, so they are easily damaged during these characterization processes, inevitably impacting the validity of the results from such experiments.[2–4] In addition, many of above-mentioned techniques require cutting the sample into thin slices and therefore are destructive to the sample.

Fourier transform infrared (FTIR) spectroscopy uses much less destructive IR light (<500 meV photo energy) and can deliver detailed qualitative and quantitative chemical information with minimum or no sample damage. Over the past decades, the FTIR or micro-FTIR microscope has been used in the research and development environment to probe the radiation and baking induced chemical change in resist materials.[5–9] These FTIR results are often combined with EUV absorption and outgassing results for a comprehensive understanding of photoreaction mechanism in various resists.

However, the spatial resolution of conventional FTIR (or IR) microscope is limited by diffraction of the long wavelength of the incident IR light, typically a few hundred nanometers or micrometers. Such a diffraction limit prevents the use of the conventional FTIR technique to acquire spatially resolved composition information at the scale relevant to scale of interest in EUV lithographic patterns, typically on the scale of 10^0 to 10^1 nm. Atomic force microscopy (AFM), on the other hand, has excellent spatial resolution (down to sub-nanometer). If a broadband IR beam can be coupled onto an AFM probe, IR spectroscopy can achieve spatial resolution down to the nanometer range. Such coupling can be realized by focusing a broadband coherent IR light onto a metal-covered AFM probe, which creates a plasmonic enhancement of the IR field near the tip apex. Such a near-field enhancement decays exponentially away from the tip apex in all directions with a characteristic decay length on the order of the tip radius (typically 10 to 15 nm). This near-field enhancement circumvents the diffraction limit and provides surface sensitivity and nanometric spatial resolution to chemical-sensitive IR spectroscopy.[10–14] Recently, such a nano-FTIR technique has been utilized to study the nanoscale structure and properties of many soft materials, including polymer and protein self-assembly layers.[15–18] A similar technique termed atomic force microscopy-infrared (AFM-IR) was also used to access photoinduced modification of resist after the laser pulse, but no spatial resolved information was demonstrated yet.[19]

Here we report the first proof-of-concept experiment of the use of nano-FTIR to characterize the chemical gradient at the tens of nanometer length scale on a Lam's proprietary dry-deposited metal-containing EUV resist.[1] The modulation of the chemical composition was observed on line/space patterns, which informed the local chemical transformation induced by exposure. Our results demonstrate the capability of this spectro-microscopy technique to provide chemical information on EUV resists at the sub-micrometer length scale. Improvement is needed to further reduce the spatial resolution and enable meaningful resist characterization at relevant length scales.

2 Experimental

2.1 *Sample Preparation*

Au-coated Si substrates were used in these experiments. They were prepared using a commercial
thermal evaporator system, Denton DV-502A. The evaporation was performed at $\sim 10^{-7}$ torr pressure and room temperature. The film thickness was monitored using a quartz crystal microbalance. Prior to the deposition of a 70-nm Au film, a 3-nm Cr film was evaporated onto Si substrates as an adhesion layer. Other details of evaporation can be found in our previous work.[15,20]

Metal-containing photoresists (~70 nm) were deposited onto the Au-coated Si substrates using Lam's proprietary dry deposition methods.[1] The PR thickness of 70 nm was thicker than that used in practical EUV exposures to enhance the signal-to-noise ratio (SNR) for the proof-of-concept experiments. A mercury UV lamp was used to generate "fully exposed" resist films by exposing a piece of above-mentioned film for 5 min. Such a treatment completely removed the photo-sensitive alkyl groups and crosslink the metal-containing clusters, as evidenced by the attenuated total reflectance (ATR)-FTIR results. Both the electron beam and EUV photons induce a similar chemical reaction.[21]

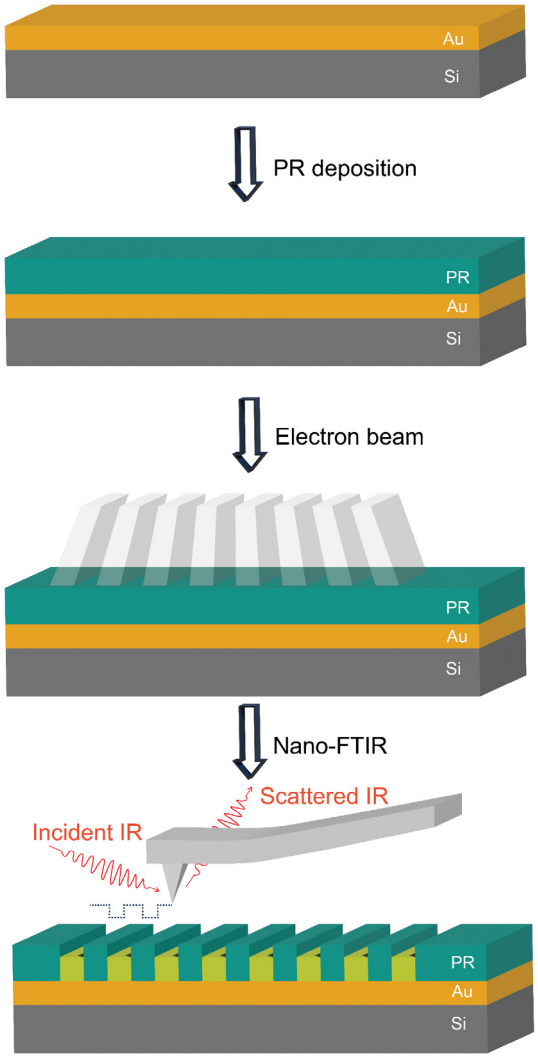

Fig. 1 Schematic workflow from photoresist deposition to nano-FTIR measurement.

The line/space patterns were created using the scanning e-beam in a bench-top SEM (Phenom 1048 Pro-X, Nanoscience Instruments). It was found that, in this benchtop SEM, at a magnification <750× and under EDS mapping mode, the spot size of the e-beam (~300 nm) is not large enough to cover the entire map, leaving an unexposed area between the exposed lines and thus creating line/space patterns. Such a method enables us to quickly produce many line/space patterns to test the proof-of-concept experiments. The accelerating voltage, magnification, and exposure time that we used in this study to pattern the PR film are 5 kV, 500×, and 1 min, respectively.

The workflow from deposition to SEM patterning to nano-FTIR measurements is summarized in Fig. 1.

2.2 *ATR-FTIR Measurement*

The ATR-FTIR measurements were conducted by a Thermo Nicolet iS50 FTIR spectrometer with a diamond crystal ATR module. The spectra were collected with 4 cm^{-1} resolution in the spectral range from 4000 to 400 cm^{-1} averaging over 64 scans and normalized to the incident light intensity. ATR-FTIR spectra on large areas of exposed and unexposed PR films were compared to decide the most informative wavenumber range that should be focused on in the subsequent nano-FTIR characterization.

2.3 *Nano-FTIR Measurement*

Synchrotron based nano-FTIR [also known as synchrotron infrared nano spectroscopy (SINS)] measurements were performed at beamline 2.4 of the Advanced Light Source at the Lawrence Berkeley National Laboratory, using a neaSNOM (Neaspec, Germany) system. The measurements were performed under an inert environment with a constant N_2 purge and <5% relative humidity. To minimize tip contamination, the IrPt-coated AFM tip was operated in a noncontact tapping mode at the fundamental resonance frequency of the cantilever (250 to 350 kHz) with a free oscillation amplitude ranging from 70 to 80 nm and an amplitude set point of ~85%. A mercury–cadmium–telluride (MCT) detector and copper-doped germanium (Ce:Gu) detector were used to collect high energy (1000 to 2000 cm^{-1}) and low energy (400 to 1000 cm^{-1}) IR photons, respectively. The scattered near-field IR signal is further filtered by a lock-in amplifier tuned to the second and higher harmonics of the cantilever oscillation to separate it from the far field non-local scattering background.

In a typical nano-FTIR experiment, AFM topography with white-light imaging measurements was first performed, and the unexposed/exposed region were identified based on the contrast of the height, phase, and second harmonic IR scattering amplitude. After the AFM scan, the tip followed the path across predefined line patterns while taking the spectrum at each point. The line profiles using different detectors were performed separately on the same sample. At each point, the spectra were collected with 8 cm^{-1} resolution averaging over 24 scans and normalized to the incident light intensity measured on the bare Au-coated Si substrate.

The complex-valued near-field spectrum is derived from a Fourier transform of the interferogram. The Fourier components are expressed as real spectral amplitude "A" and phase "$\varnothing$," both normalized to reference spectra:

$$A_i(v) = \frac{A_i^{\text{sample}}(v)}{A_i^{\text{reference}}(v)}, \quad \varnothing_i(v) = \varnothing_i^{\text{sample}}(v) - \varnothing_i^{\text{reference}}(v),$$

where v is the wavenumber and the reference spectra were collected on bare Au-coated Si substrates. The nano-FTIR spectra displayed throughout the paper is the phase φ_2 of the scattered signal at the second harmonic of the cantilever oscillation frequency, which has been shown to be in good agreement with traditional FTIR absorption measurements.[11,12,20] Each nano-FTIR spectrum has a third order polynomial background subtracted. The negative band around 1270 cm^{-1} in all cases is likely associated with polydimethylsiloxane contamination on the AFM cantilever and tip, a material present in the gel box where the AFM tips were held.

3 Results and Discussion

3.1 *ATR-FTIR on Unexposed and Fully Exposed PR Films*

ATR-FTIR spectra were collected on large areas of unexposed and fully exposed resist films to reveal the most significant spectral difference before and after exposure, as depicted in the blue and brown traces in Fig. 2, respectively. It is worth noting that the metal oxide resist used in this study is sensitive to a variety of excitations, including EUV and UV light as well as e-beam. There may be some detailed difference in the reaction mechanism in terms of how the resist materials change under different forms of excitation, but the composition of the fully exposed film is the same, which is characterized by the removal of the alkyl group as well as crosslinking of metal oxide clusters.[21] Here, a resist film overexposed under a UV lamp was used as the fully exposed film and represents the extreme case in which all bleachable motifs are consumed.

ATR-FTIR of unexposed and exposed resist films showed three wavenumber regions with the most noticeable spectral changes: (1) 2800 to 3000 cm^{-1}; (2) 1400 to 1700 cm^{-1}; and (3) 450 to 850 cm^{-1}. Peaks in regions 1 and 2 can be attributed to C–H stretch and scissor modes, respectively.[22,23] The disappearance of peaks in these two regions indicates the complete consumption of the C_xH_y component in the resist film when overexposed. In region 3, the unexposed film exhibited distinctive fingerprint features, indicating metal-containing nano-clusters

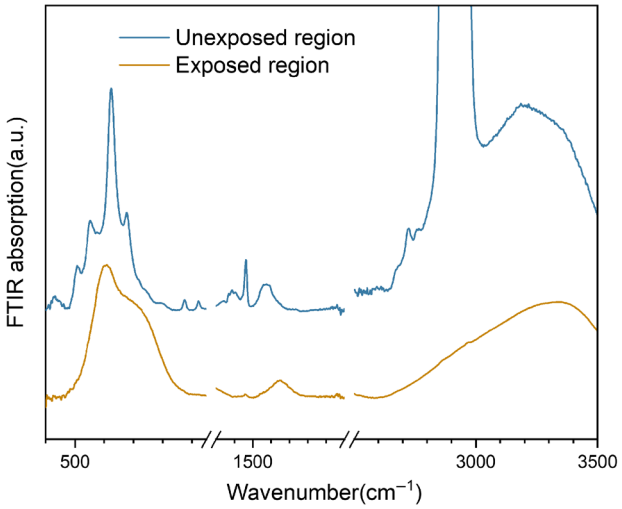

Fig. 2 ATR-FTIR spectra of unexposed (blue trace) and fully exposed (brown trace) photoresist film. The fingerprint features at the top of the C–H stretch peak is cut off from the graph to conceal the composition information of Lam's proprietary resist film.

with well-defined size and/or geometry. After exposure, these fingerprints evolved into a broadened hump with decreased intensity, characteristic of amorphous metal oxides.

The spectra difference observed in unexposed and exposed resist films suggests that the most informative features that we should monitor in the nano-FTIR characterizations are those related to C—H bonds and metal-oxygen (M–O) bonds. Because the coupling of the synchrotron IR light and the AFM tip in our experiment is optimum between 1000 and 1600 cm^{-1} and less efficient beyond 2000 cm^{-1} using the MCT detector,[12] the C—H scissor peak at 1460 cm^{-1}, instead of the most intense C—H stretch peaks at 2900 cm^{-1}, was selected in the subsequent nano-FTIR experiments.

3.2 *Nano-FTIR Line Scan across Line/Space Patterns*

Figures 3(a) and 3(d) show the AFM topography over the line-space patterns on the same resist film in two different measurements. As discussed in experimental methods, different detectors are required for the two wavenumber regions of interest, which is why the data presented here were acquired in two separate measurements. Because the resist film loses the C_xH_y component and shrinks upon exposure, the bright regions in the AFM topography image represent unexposed areas, and the valley regions were exposed.

Line scans in the C—H scissoring and M—O regions were acquired along the red arrows marked in Fig. 3(a) and 3(d), respectively. During the measurement, the AFM tip moved along the direction of the arrow while taking the FTIR spectra at a 40- to 50-nm interval. In both the C—H and M—O regions, peak intensity modulation can be seen across the line/space patterns. When the integrated intensity of peaks in both C—H and M—O regions are plotted as a function of distance, both chemical profiles track the topography height profile relatively well.

In addition, a slight redshift of C—H scissoring peak was observed at the boundary of the exposed/unexposed area. This is likely related to some intermediate chemical state in partially exposed resist materials, but more experiments are needed to verify the reproducibility of the redshift and to investigate the chemical origin of such a shift. Unfortunately, it is difficult to resolve those sharp fingerprints in the M—O region as seen in the ATR-FTIR spectrum because of limited SNR in current nano-FTIR systems.

3.3 *Discussion*

These nano-FTIR results demonstrated the feasibility of acquiring chemical profile information at a 40-nm spatial resolution, well below the optical diffraction limits of IR light. However, there

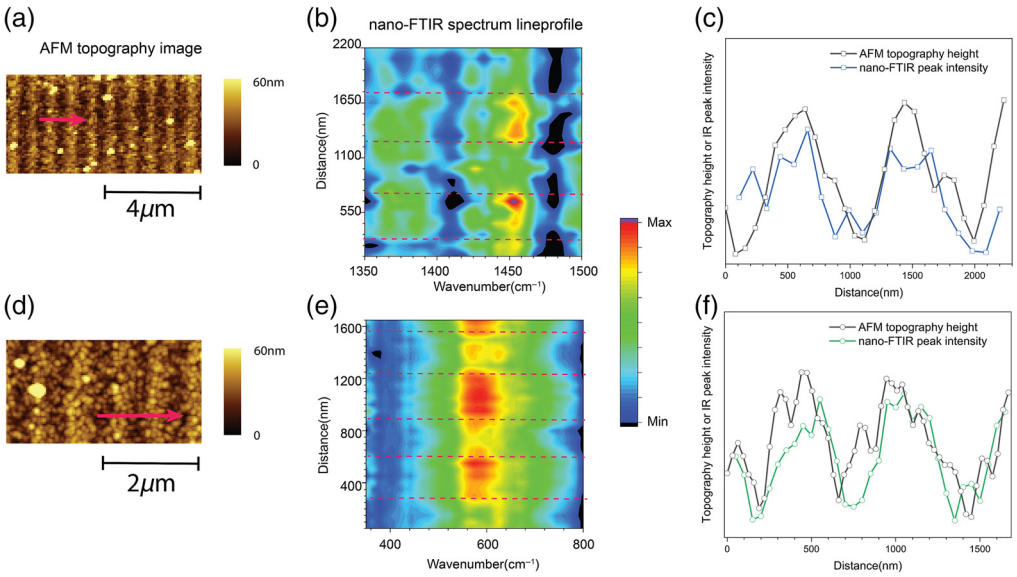

Fig. 3 (a) and (d) Images of AFM topography over the line/space pattern on the same resist film in different measurements. The scan size is 8 μm × 4 μm for (a) and 4 μm × 2 μm for (d), respectively. The grainy morphology comes from the grains of the thermally evaporated Au films underneath. The red arrows in (a) and (d) mark the positions where the subsequent line scan was acquired. (b) and (e) Corresponding color map representations of the nano-FTIR spectral intensities (arbitrary units in the color scale) of resist film across the line/space patterns in different wavenumber ranges. Red dashed lines in both color maps represent roughly the boundary position between exposed and unexposed areas. (c) The C–H scissoring peak intensity integrated from 1433 to 1467 cm^{-1} in the line scan shown in (b), overlaid on the AFM topography height profile extracted from (a). (f) The M–O peak intensity integrated from 440 to 760 cm^{-1} in the line scan shown in (e), overlaid on the AFM topography height profile extracted from (d).

are a couple of issues that need to be addressed before we can apply this technique to features with relevant sizes in the era of EUV lithography.

It was found that the Au substrate coupled with a PtIr-coated AFM tip produced the maximum enhancement of near-field optical signals, compared with other combinations that we have tested, such as Si substrate + PtIr-coated tip. More evaluation is necessary to explore other possible combinations of substrates and tip coatings. In addition, the current substrate, thermally evaporated Au films, is not smooth enough with obvious Au grains, causing interference with the delicate AFM/nano-FTIR signal.

Another obvious limitation of the current version of Nano-FTIR is the spatial resolution, which is currently limited by the apex size of the metal-coated AFM tip. The necessity of the metal coating on the AFM tip makes it extremely challenging to further shrink the apex size. The best spatial resolution recorded for this nano-FTIR technique is 15 nm,[11] which is still larger than the size relevant to the EUV lithography evaluation. In addition, the low throughput of nano-FTIR may be also an obstacle for its application as a routine characterization method.

4 Conclusion

In summary, we demonstrated the feasibility of using nano-FTIR to obtain nanoscale chemical information of nanopatterned photoresist film. The exposure removed C_xH_y species and transformed photoresist into amorphous metal oxide, as evidenced by the peak intensity change in nano-FTIR spectrums. The observed modulation of C—H and M—O peak intensity across the line/space pattern can be directly correlated to alternating exposed/unexposed areas. The nanoscale spatial resolution, chemical sensitivity, and minimal radiation damage make nano-FTIR a promising candidate for the fundamental study of material properties relevant to EUV lithography. However, significant improvement may be needed before this novel spectromicroscopy technique can be more useful in the research and development of EUV photoresist materials.

Acknowledgments

This project was funded by Lam Research Corporation. This research used resources of the Advanced Light Source, a DOE Office of Science User Facility under contract no. DE-AC02-05-CH11231. Nano-FTIR was performed at beamline 2.4 in ALS, and ATR-FTIR was per-formed at the Molecular Foundry, supported by the DOE Office of Basic Energy Sciences under the same contract number. Xiao Zhao was supported by an NSF-BSF grant number 1906014. Miquel Salmeron was supported by U.S. Department of Energy, Office of Science, Office of Basic Energy Sciences, Materials Sciences and Engineering Division under Contract No. DE-AC02-05-CH11231 program Unlocking Chemical Circularity in Recycling by Controlling Polymer Reactivity Across Scales.

References

1. R. S. Wise, "Breaking stochastic tradeoffs with a dry deposited and dry developed EUV photoresist system," *Proc. SPIE* **11612**, 1161203 (2021).
2. G. Conti et al., "Chemical and structural characterization of EUV photoresists as a function of depth by standing-wave x-ray photoelectron spectroscopy," *J. Micro/Nanopatterning, Mater. Metrol.* **20**, 034603 (2021).
3. H. X. Wang et al., "X-ray-induced fragmentation of imidazolium-based ionic liquids studied by soft X-ray absorption spectroscopy," *J. Phys. Chem. Lett.* **9**, 785–790 (2018).
4. Z. J. W. A. Leijten et al., "Quantitative analysis of electron beam damage in organic thin films," *J. Phys. Chem. C* **121**, 10552–10561 (2017).
5. P. Rosenthal et al., "Advanced FTIR technology for the chemical characterization of product wafers," in *AIP Conf. Proc.*, American Institute of Physics, pp. 553–557 (2001).
6. R. A. Carpio et al., "Advanced FTIR techniques for photoresist process characterization," *Proc. SPIE* **3050**, 545–556 (1997).
7. T. R. Pampalone, A. M. Gilfillan, and P. J. Zanzucchi, "Fourier Transform Infrared (FTIR) analysis of photoresist films on silicon wafers," *J. Electrochem. Soc.* **133**, 1917–1922 (1986).
8. S. Grzeskowiak et al., "Analytical techniques for mechanistic characterization of EUV photoresists," *Proc. SPIE* **10146**, 101462C (2017).
9. P. De Schepper et al., "H2 plasma and neutral beam treatment of EUV photoresist," *Proc. SPIE* **9428**, 39–46 (2015).
10. F. Mooshammer et al., "Quantifying nanoscale electromagnetic fields in near-field microscopy by Fourier demodulation analysis," *ACS Photonics* **7**, 344–351 (2020).
11. H. A. Bechtel et al., "Synchrotron infrared nano-spectroscopy and-imaging," *Surf. Sci. Rep.* **75**, 100493 (2020).
12. H. A. Bechtel et al., "Ultrabroadband infrared nanospectroscopic imaging," *Proc. Natl. Acad. Sci. U. S. A.* **111**, 7191–7196 (2014).
13. F. Huth et al., "Nano-FTIR absorption spectroscopy of molecular fingerprints at 20 nm spatial resolution," *Nano Lett.* **12**, 3973–3978 (2012).
14. A.V. Zayats and D. Richards, *Nano-Optics and Near-Field Optical Microscopy*, Artech House (2009).
15. X. Zhao et al., "*In vitro* investigation of protein assembly by combined microscopy and infrared spectroscopy at the nanometer scale," *Proc. Natl. Acad. Sci. U. S. A.* **119**, e2200019119 (2022).
16. L. Mester et al., "Subsurface chemical nanoidentification by nano-FTIR spectroscopy," *Nat. Commun.* **11**, 1–10 (2020).
17. O. Khatib et al., "Graphene-based platform for infrared near-field nanospectroscopy of water and biological materials in an aqueous environment," *ACS Nano* **9**, 7968–7975 (2015).
18. I. Amenabar et al., "Structural analysis and mapping of individual protein complexes by infrared nanospectroscopy," *Nat. Commun.* **4**, 2890 (2013).
19. C. B. Marble, K. S. Marble, and V. V. Yakovlev, "Nanoscale optical assessment of photochemical changes of SU-8 photoresist induced by ultrashort near-IR optical excitation," *Appl. Phys. A* **126**, 808 (2020).

20. Y.-H. Lu et al., “Infrared nanospectroscopy at the graphene-electrolyte interface,” *Nano Lett.* **19**, 5388–5393 (2019).
21. T. G. Oyama, A. Oshima, and S. Tagawa, “Estimation of resist sensitivity for extreme ultraviolet lithography using an electron beam,” *AIP Adv.* **6**, 085210 (2016).
22. N. Thakur et al., “Stability studies on a sensitive EUV photoresist based on zinc metal oxoclusters,” *J. Micro/Nanolithogr. MEMS MOEMS* **18**, 043504 (2019).
23. D. E. Gray, *American Institute of Physics (AIP). Handbook*, American Institute of Physics (1963).